$\Lambda(1405)$ production in the process $\chi_{c0}(1P) \to \bar{\Lambda}\Sigma\pi$

Li-Juan Liu,[1] En Wang,[1,*] Ju-Jun Xie,[2,†] Kai-Lan Song,[1] and Jing-Yu Zhu[1]

[1]*School of Physics and Engineering, Zhengzhou University, Zhengzhou, Henan 450001, China*
[2]*Institute of Modern Physics, Chinese Academy of Sciences, Lanzhou 730000, China*

(Received 16 June 2018; published 18 December 2018)

We have performed a theoretical study on the process $\chi_{c0}(1P) \to \bar{\Lambda}\Sigma\pi$, by taking into account the final-state interactions of $\pi\Sigma$ and $\pi\bar{\Lambda}$ based on the chiral unitary approach. As the isospin filters of $I = 0$ in the $\pi\Sigma$ channel and $I = 1$ in the $\pi\bar{\Lambda}$ channel, this process can be used to study the molecular structure of the $\Lambda(1405)$ resonance and to test the existence of the predicted states $\Sigma(1380)$ and $\Sigma(1430)$ with spin parity $J^P = 1/2^-$. Our results show that there is a peak around 1350–1400 MeV and a cusp around the $\bar{K}N$ threshold in the $\pi\Sigma$ invariant mass distribution, which should be the important feature of the molecular state $\Lambda(1405)$. We also find a peak around 1380 MeV and a cusp around the $\bar{K}N$ threshold in the $\pi\bar{\Lambda}$ invariant mass distribution, which are associated to the $\Sigma(1380)$ and $\Sigma(1430)$ resonances.

DOI: 10.1103/PhysRevD.98.114017

I. INTRODUCTION

The nature of the baryon resonances is one of the important issues in hadron physics [1,2]. There are many facilities, such as BESIII, LHCb, Belle, etc., that have presented a lot of information about baryon resonances, which provides a good platform on which to extract the baryon properties. On the other hand, the theoretical works go parallel, most of the existing states can be well described, and some predictions of the effective theories have been confirmed experimentally.

One of the important predictions is the existence of two poles of the $\Lambda(1405)$ state, which were first reported in Ref. [3], discussed in detail in Ref. [4], and later on confirmed in all theories using the chiral unitary approach [5–17]. The experimental confirmation came from the work of Ref. [18] and the analysis of Ref. [19], but other experiments have come to confirm it, too (see Refs. [20,21] for more details). The low pole mainly couples to the $\pi\Sigma$ channel, and the high one couples strongly to the $\bar{K}N$ channel [20,22]. In addition, many theoretical works about $\Lambda(1405)$ production induced by photon [20,22–26], pion [27], kaon [19,28–32], neutrino [33], proton-proton collision [24,34,35], and heavy meson decay [36–41] were carried out to clarify the molecular nature of the $\Lambda(1405)$ resonance. However, it is problematic to extract the $\Lambda(1405)$ in some conventional reactions involving $\bar{K}N$ or $\pi\Sigma$ final states, which may mix $I = 0$ and $I = 1$ contributions.

To further understand the molecular structure of the $\Lambda(1405)$ state, we investigate the process $\chi_{c0}(1P) \to \bar{\Lambda}\Sigma\pi$, by considering the final-state interaction of $\pi\Sigma$, which will dynamically generate the two poles of the $\Lambda(1405)$ state in the chiral unitary approach. The $\chi_{c0}(1P)$, with $I^G(J^{PC}) = 0^+(0^{++})$, is a $c\bar{c}$ state and blind to SU(3), hence behaving like an SU(3) singlet. Since the outgoing particle $\bar{\Lambda}$ has isospin $I = 0$, the $\pi\Sigma$ system must have isospin $I = 0$, to combine to the isospin $I = 0$ of the $\chi_{c0}(1P)$. Thus, this process is a good filter of isospin that guarantees that the $\pi\Sigma$ system will be in $I = 0$. Besides, the lower $\Lambda(1405)$ pole couples strongly to the $\pi\Sigma$ channel, so the $\pi\Sigma$ final state in this process is an ideal channel to study the molecular structure of the $\Lambda(1405)$ state.

The π and $\bar{\Lambda}$ can also undergo final-state interaction, and the isospin of $\pi\bar{\Lambda}$ system is $I = 1$, which together with the Σ gives rise to the isospin $I = 0$ of χ_{c0}. It should be noted that a baryon resonance around the $\bar{K}N$ threshold with $J^P = 1/2^-$, strangeness $S = -1$, and isospin $I = 1$ was predicted in the chiral unitary approach [3,4] [we label this state as $\Sigma(1430)$ in the following] and can couple to the $\pi\Lambda$ channel. It was also suggested to search for this state in the process $\chi_{c0} \to \bar{\Sigma}\Sigma\pi$ in Ref. [42]. In addition, a Σ^* state with $J^P = 1/2^-$, mass $M \sim 1380$ MeV, and width $\Gamma \sim 120$ MeV [we label this state as $\Sigma(1380)$ in the following] has been predicted in the pentaquark picture [43]. The role of the $\Sigma(1380)$ was investigated in the processes of J/ψ decay [44,45], $K^- p \to \Lambda\pi^+\pi^-$ [46,47], $\Lambda p \to \Lambda p\pi^0$ [48], $\Lambda_c^+ \to \eta\pi^+\Lambda$ [49], and so on. The χ_{c0} can also decay into a Σ and the intermediate resonance $\bar{\Sigma}(1380)$ in the s wave, and then the $\bar{\Sigma}(1380)$ decays into the $\pi\bar{\Lambda}$ states in the s

*wangen@zzu.edu.cn
†xiejujun@impcas.ac.cn

wave. As a result, for the s-wave final-state interaction of $\pi\bar{\Lambda}$, we will consider the mechanism of the $\bar{\Sigma}(1430)$ dynamically generated in the chiral unitary approach and the contribution of the intermediate resonance $\bar{\Sigma}(1380)$.[1] In this way, the shape of the $\pi\bar{\Lambda}$ mass distribution of this process can be helpful to test the existences of the $\Sigma(1430)$ and $\Sigma(1380)$ resonances [21,45]. It should be noted that the $\Sigma(1430)$ and $\Sigma(1380)$ resonances are assumed to be the members of the SU(3) octet in this work, since the antisinglet and antidecuplet of the $\pi\bar{\Lambda}$ system are suppressed in the $\chi_{c0} \to \bar{\Lambda}\Sigma\pi$ reaction.

In addition, the Lattice QCD groups have also calculated the mass of the Σ^* with $J^P = 1/2^-$. For instance, the mass of the lowest Σ^* ($J^P = 1/2^-$) is predicted to be about 1.2 GeV in Ref. [50] and 1.6–1.8 GeV in Refs. [51,52], both of which are inconsistent with the masses of $\Sigma(1430)$ and $\Sigma(1385)$. Thus, searching for the Σ^* state with $J^P = 1/2^-$ experimentally could distinguish the different theoretical predictions.

This paper is organized as follows. In Sec. II, we will give the formalism of mechanisms. In Sec. III, we will present our results and discussions. Finally, the conclusion will be given in Sec. IV.

II. FORMALISM

In this section, we will describe the reaction mechanism for the process $\chi_{c0}(1P) \to \bar{\Lambda}\Sigma\pi$.

A. Model of $\chi_{c0}(1P) \to \bar{\Lambda}\Sigma\pi$

In the first step, $\chi_{c0}(1P)$ can decay into the final states $\bar{\Lambda}\Sigma\pi$ directly in the tree level, as depicted in Fig. 1(a). Then, the final particles $\pi\Sigma$ can undergo the final-state interaction, which will dynamically generate the resonance $\Lambda(1405)$, as depicted in Fig. 1(b).

For the mechanism of the $\pi\Sigma$ final-state interaction, we must take into account that, in the first step, one can produce the other meson-baryon pairs that couple to the same $\pi\Sigma$ quantum numbers, then reach the final $\pi\Sigma$ through rescattering. Since χ_{c0} behaves like an SU(3) singlet and $\bar{\Lambda}$ is an SU(3) antioctet, the $\pi\Sigma$ system should be in an SU(3) octet, which will give rise to the same quantum numbers as $\Lambda(1405)$. Since both π and Σ belong to the members of the SU(3) octet, we have the representation for $8(\pi) \otimes 8(\Sigma)$ going to the 8^s (symmetry) and 8^a (antisymmetry). With the SU(3) isoscalar factors given by the Particle Data Group [21], tabulated in Table I, we can obtain the weights h_i in the isospin basis of this states, which go into the primary production of each meson-baryon channel and stand for the weights of the transition $\chi_{c0} \to \bar{\Lambda}PB$ ($PB = \bar{K}N$, $\pi\Sigma$, $\eta\Lambda$, ΞK),

[1]We do not consider the contribution of the intermediate $\bar{\Sigma}(1385)$ with $J^P = 3/2^-$ in $\pi\bar{\Lambda}$ system, because the $\bar{\Sigma}(1385)$, as the SU(3) antidecuplet, together with the SU(3) octet state Σ, cannot give rise to the SU(3) singlet state χ_{c0}, and its contribution will be suppressed.

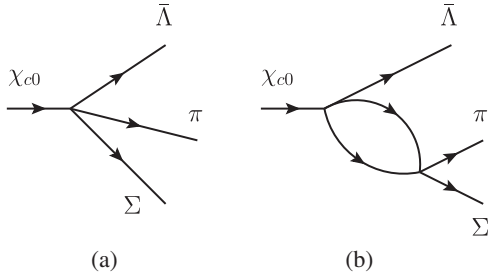

FIG. 1. Diagrams for $\chi_{c0} \to \bar{\Lambda}\Sigma\pi$ decay: (a) direct $\bar{\Lambda}\Sigma\pi$ vertex at tree level and (b) final-state interaction of $\pi\Sigma$.

$$h_{\bar{K}N} = \sqrt{\frac{1}{10}}\tilde{D} + \sqrt{\frac{1}{2}}\tilde{F}, \qquad h_{\pi\Sigma} = -\sqrt{\frac{3}{5}}\tilde{D},$$
$$h_{\eta\Lambda} = -\sqrt{\frac{1}{5}}\tilde{D}, \qquad h_{K\Xi} = -\sqrt{\frac{1}{10}}\tilde{D} + \sqrt{\frac{1}{2}}\tilde{F}, \quad (1)$$

where $\tilde{D}$ and $\tilde{F}$ are unknown parameters.

The interaction of the octet pseudoscalar mesons and the octet $1/2^+$ baryons, which can dynamically generate the $\Lambda(1405)$, has been studied within the chiral unitary approach in Refs. [3,6,53]. In Ref. [22], a new strategy to extract the positions of the two poles of $\Lambda(1405)$ from $\pi\Sigma$ photoproduction experimental data was done, based on small modifications of the unitary chiral perturbation theory amplitude, which will be adopted in this work. Because the thresholds of the channels $\eta\Lambda$ and $K\Xi$ lay far above the energies that we consider in this work, and their effect can be effectively reabsorbed in the subtraction constants, as discussed in Refs. [20,22], we do not consider these two channels in following calculations.

In addition to the $\pi\Sigma$ final-state interaction, the states π and $\bar{\Lambda}$ can also undergo the final-state interaction in the process of $\chi_{c0} \to \bar{\Lambda}\Sigma\pi$, as depicted in Fig. 2. In this case, we get the weights for different channels from Ref. [42],

$$\tilde{h}_{K\bar{N}} = -\sqrt{\frac{3}{8}}\tilde{D} + \sqrt{\frac{1}{6}}\tilde{F},$$
$$\tilde{h}_{\pi\bar{\Sigma}} = \sqrt{\frac{2}{3}}\tilde{F}, \qquad \tilde{h}_{\pi\bar{\Lambda}} = \sqrt{\frac{1}{5}}\tilde{D}, \qquad \tilde{h}_{\eta\bar{\Sigma}} = \sqrt{\frac{1}{5}}\tilde{D},$$
$$\tilde{h}_{\bar{K}\,\bar{\Xi}} = -\sqrt{\frac{3}{8}}\tilde{D} + \sqrt{\frac{1}{6}}\tilde{F}, \quad (2)$$

where the parameters $\tilde{D}$ and $\tilde{F}$ are same as those of Eq. (1).

TABLE I. SU(3) isoscalar coefficients for the $\langle\bar{\Lambda}|MB\rangle$ matrix elements.

$\bar{\Lambda}$	$\bar{K}N$	$\pi\Sigma$	$\eta\Lambda$	$K\Xi$
$\tilde{D}$	$\sqrt{\frac{1}{10}}$	$-\sqrt{\frac{3}{5}}$	$-\sqrt{\frac{1}{5}}$	$-\sqrt{\frac{1}{10}}$
$\tilde{F}$	$\sqrt{\frac{1}{2}}$	0	0	$\sqrt{\frac{1}{2}}$

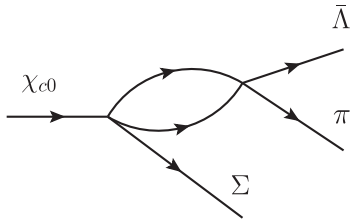

FIG. 2. The s-wave final-state interaction of $\pi\bar{\Lambda}$ in the process $\chi_{c0} \to \bar{\Lambda}\Sigma\pi$.

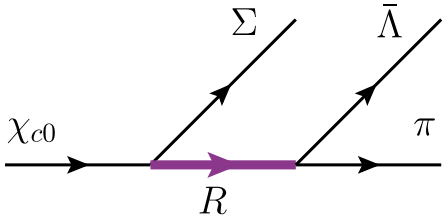

FIG. 3. The mechanism of the intermediate resonance $\bar{\Sigma}(1380)$ in the $\pi\bar{\Lambda}$ channel in the process $\chi_{c0} \to \bar{\Lambda}\Sigma\pi$.

As predicted in Refs. [3,4], the $\pi\bar{\Lambda}$ system with isospin $I = 1$ can undergo the s-wave final-state interaction, which will dynamically generate a cusp structure around the $\bar{K}N$ threshold, associated to the $\Sigma(1430)$ resonance. Taking into account the s-wave final-state interaction, the total amplitude for the process $\chi_{c0} \to \bar{\Lambda}\Sigma\pi$ is

$$\begin{aligned}\mathcal{M} &= V_p\left[h_{\pi\Sigma} + \sum_i h_i G_i(M_{\pi\Sigma}) t_{i,\pi\Sigma}(M_{\pi\Sigma})\right] \\ &\quad + \tilde{V}_p \sum_j \tilde{h}_j G_j(M_{\pi\bar{\Lambda}}) t_{j,\pi\bar{\Lambda}}(M_{\pi\bar{\Lambda}}) \\ &= \mathcal{M}_{\text{tree}} + \mathcal{M}_{\pi\Sigma} + \mathcal{M}_{\pi\bar{\Lambda}}, \end{aligned} \tag{3}$$

where the loop function G and the transition amplitude t of the $\pi\Sigma$ final-state interaction are taken from Refs. [22,42]. $M_{\pi\Sigma}$ and $M_{\pi\bar{\Lambda}}$ are the invariant masses of the $\pi\Sigma$ and $\pi\bar{\Lambda}$, respectively. In this work, we work with $R = \tilde{F}/\tilde{D}$ and include the weight $\tilde{D}$ of Eqs. (1) and (2) in the V_p and $\tilde{V}_p$ factors, as done in Ref. [42].

In Eq. (3), the amplitude for the tree level of Fig. 1(a) is

$$\mathcal{M}_{\text{tree}} = V_p h_{\pi\Sigma}. \tag{4}$$

If we consider the transition $\chi_{c0} \to \Sigma P\bar{B}$ ($P\bar{B} = K\bar{N}$, $\pi\bar{\Sigma}$, $\pi\bar{\Lambda}$, $\eta\bar{\Sigma}$, $\bar{K}\,\bar{\Xi}$), the amplitude for the tree level can also be given as

$$\mathcal{M}_{\text{tree}} = \tilde{V}_p \tilde{h}_{\pi\bar{\Lambda}}. \tag{5}$$

Combing Eqs. (4) and (5), we can obtain that $\tilde{V}_p = V_p \times (h_{\pi\Sigma}/\tilde{h}_{\pi\bar{\Lambda}}) = -\sqrt{3}V_p$. Now, the amplitude of Eq. (3) can be rewritten as

$$\begin{aligned}\mathcal{M} &= V_p\left[h_{\pi\Sigma} + \sum_i h_i G_i(M_{\pi\Sigma}) t_{i,\pi\Sigma}(M_{\pi\Sigma})\right. \\ &\quad \left. -\sqrt{3}\sum_j \tilde{h}_j G_j(M_{\pi\bar{\Lambda}}) t_{j,\pi\bar{\Lambda}}(M_{\pi\bar{\Lambda}})\right] \\ &= V_p(h_{\pi\Sigma} + T_{\pi\Sigma} + T_{\pi\bar{\Lambda}}). \end{aligned} \tag{6}$$

B. Contribution from $\Sigma(1380)$ with $J^P = 1/2^-$

In addition to the s-wave interaction, the $\pi\bar{\Lambda}$ states can also couple to the $\bar{\Sigma}(1380)$ state with $J^P = 1/2^+$ in the s wave, as depicted in Fig. 3. The contribution of intermediate resonance $\bar{\Sigma}(1380)$ should add coherently to Eq. (6)[2] as

$$\mathcal{M} = V_p(h_{\pi\Sigma} + T_{\pi\Sigma} + T_{\pi\bar{\Lambda}} + T_{\Sigma(1380)}), \tag{7}$$

$$T_{\Sigma(1380)} = \frac{\alpha M_{\Sigma(1380)}}{M_{\pi\bar{\Lambda}} - M_{\Sigma(1380)} + i\Gamma_{\Sigma(1380)}/2}, \tag{8}$$

where the normalization α stands for the amplitude strength, which will be chosen to provide a sizeable effect of the intermediate resonance $\bar{\Sigma}(1380)$. In this work, we take $M_{\Sigma(1380)} = 1380$ MeV, $\Gamma_{\Sigma(1380)} = 120$ MeV as fitted in Ref. [46].

With the amplitude of Eq. (7), the invariant mass distribution of $\chi_{c0}(1P) \to \bar{\Lambda}\Sigma\pi$ can be written as

$$\frac{d\Gamma}{dM_{\pi\Sigma}^2 dM_{\pi\bar{\Lambda}}^2} = \frac{1}{(2\pi)^3}\frac{4M_\Sigma M_\Lambda}{32M_{\chi_{c0}}^3}|\mathcal{M}(M_{\pi\Sigma}, M_{\pi\bar{\Lambda}})|^2. \tag{9}$$

For a given value of $M_{\pi\Sigma}^2$, the range of $M_{\pi\bar{\Lambda}}^2$ is defined as

$$\begin{aligned}(M_{\pi\bar{\Lambda}}^2)_{\max} &= (E_\pi^* + E_{\bar{\Lambda}}^*)^2 - \left(\sqrt{E_\pi^{*2} - m_\pi^2} - \sqrt{E_{\bar{\Lambda}}^{*2} - m_\Lambda^2}\right)^2, \\ (M_{\pi\bar{\Lambda}}^2)_{\min} &= (E_\pi^* + E_{\bar{\Lambda}}^*)^2 - \left(\sqrt{E_\pi^{*2} - m_\pi^2} + \sqrt{E_{\bar{\Lambda}}^{*2} - m_\Lambda^2}\right)^2; \end{aligned} \tag{10}$$

here, $E_\pi^* = (M_{\pi\Sigma}^2 - M_\Sigma^2 + m_\pi^2)/2M_{\pi\Sigma}$ and $E_{\bar{\Lambda}}^* = (M_{\chi_{c0}}^2 - M_{\pi\Sigma}^2 - M_\Lambda^2)/2M_{\pi\Sigma}$ are the energies of π and $\bar{\Lambda}$ in the rest frame of the $\pi\Sigma$ system.

III. RESULT AND DISCUSSIONS

Before presenting the results for the process $\chi_{c0}(1P) \to \bar{\Lambda}\Sigma\pi$, we show the modulus squared of the amplitudes

[2]Although the $\Sigma(1380)$ is predicted in pentaquark picture [43], for simplicity, we use the Breit-Wigner form for its contribution, as used in Refs. [46–49].

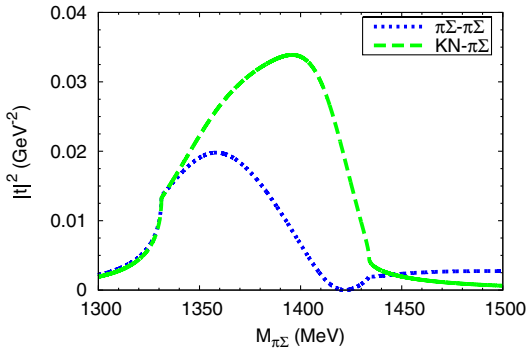

FIG. 4. Modulus squared of the amplitudes $|t_{\bar{K}N,\pi\Sigma}|^2$ and $|t_{\pi\Sigma,\pi\Sigma}|^2$ in $I = 0$.

$|t_{\bar{K}N,\pi\Sigma}|^2$ and $|t_{\pi\Sigma,\pi\Sigma}|^2$ in $I = 0$ in Fig. 4, from which we can see that the peak of the $\pi\Sigma \to \pi\Sigma$ amplitude mainly comes from the lower pole, while the one of the $\bar{K}N \to \pi\Sigma$ amplitude comes from the higher pole. In Fig. 5, we present the modulus squared of the transition amplitudes $|t|^2$ in $I = 1$. As we can see, a clear cusp structure around the $\bar{K}N$ threshold is found, the same as in Refs. [22,42].

As we do not know the exact value of $R(= \tilde{F}/\tilde{D})$ and the production weights of $\bar{K}N$ and $\pi\Sigma$ are expected to be same magnitude, we will vary the R from -2 to 2, as done in Ref. [42]. First, we take $R = 1$, and $\alpha = 0.06$ of the normalization in Eq. (8), which gives rise to a sizeable effect of intermediate $\bar{\Sigma}(1380)$. In Fig. 6, up to an arbitrary normalization of V_p, we show the $\pi\Sigma$ invariant mass distribution, in which the term of $\pi\Sigma$ final-state interaction (labeled as $T_{\pi\Sigma}$) gives rise to a peak around 1410 MeV, and the peak moves to low energy because of the interference with the tree-level term (labeled as "tree"). We also present the $\pi\Sigma$ invariant mass distribution with different values of α in Fig. 7, which shows that the contribution from the intermediate $\bar{\Sigma}(1380)$ resonance does not significantly affect the peak position of the $\pi\Sigma$ mass distribution.

The $\pi\Sigma$ invariant mass distribution with different values of R, varying from -2 to 2, is shown in Fig. 8, in which we can see that as the ratio R decreases the peak position of the

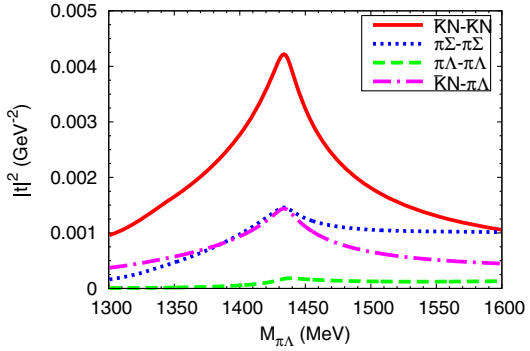

FIG. 5. Modulus squared of the amplitudes $|t_{\bar{K}N,\bar{K}N}|^2$, $|t_{\pi\Sigma,\pi\Sigma}|^2$, $|t_{\pi\Lambda,\pi\Lambda}|^2$, and $|t_{\bar{K}N,\pi\Lambda}|^2$.

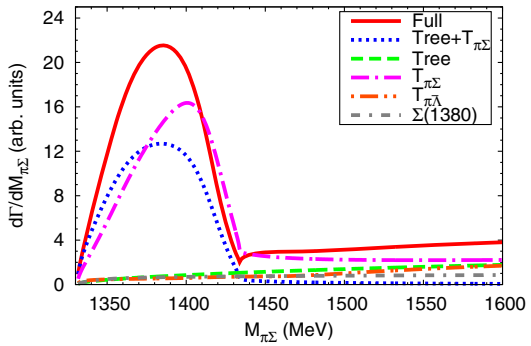

FIG. 6. The $\pi\Sigma$ mass distribution of the process $\chi_{c0} \to \bar{\Lambda}\Sigma\pi$. The curve labeled "full" shows the result of all the contributions as given by Eq. (7); the curves labeled "Tree," "$T_{\pi\Sigma}$," "$T_{\pi\bar{\Lambda}}$," and "$\bar{\Sigma}(1380)$" correspond to the contributions of the tree level [Fig. 1(a)], the $\pi\Sigma$ final-state interaction [Fig. 1(b)], the contribution of the $\bar{\Sigma}(1430)$ generated in the s-wave $\pi\bar{\Lambda}$ final-state interaction (Fig. 2), and the intermediate resonance $\bar{\Sigma}(1380)$ (Fig. 3), respectively. Finally, the curve labeled as "Tree + $T_{\pi\Sigma}$" represents the total contribution of the tree level [Fig. 1(a)] and the $\pi\Sigma$ final-state interaction [Fig. 1(b)].

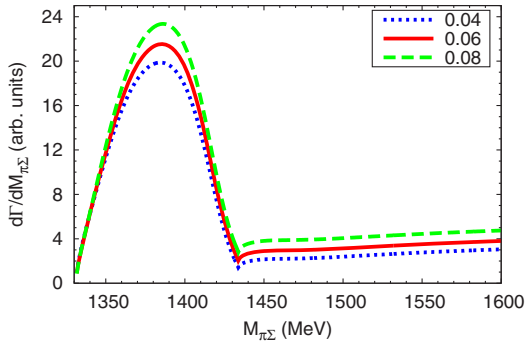

FIG. 7. The $\pi\Sigma$ mass distribution of the process $\chi_{c0} \to \bar{\Lambda}\Sigma\pi$ for different values of α of Eq. (8).

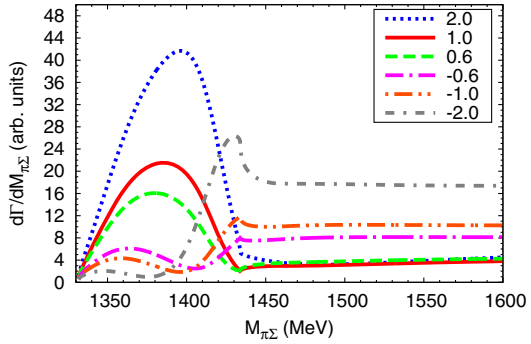

FIG. 8. The $\pi\Sigma$ mass distribution of the process $\chi_{c0} \to \bar{\Lambda}\Sigma\pi$ for different values of the ratio R.

$\Lambda(1405)$ in the $\pi\Sigma$ mass distribution moves to the region of low energies, and a cusp structure around $\bar{K}N$ threshold appears. Indeed, the value of R can be larger than 2 or less than -2, and the peak of the $\pi\Sigma$ invariant mass distribution

will vary from 1360 MeV, the position of the peak in $t_{\pi\Sigma,\pi\Sigma}$, to 1400 MeV, the one in $t_{\bar{K}N,\pi\Sigma}$, as shown in Fig. 4.

As discussed in Refs. [54–57], one of the defining features associated to the molecular states that couple to several hadron-hadron channels is that one can find a strong and unexpected cusp at the threshold of the channels corresponding to the main component of the molecular state, and one of the examples is the observations of the cusp, associated to the molecular state $X(4160)$, in the $B^+ \to J/\psi\phi K^+$ decay [55]. The peak and the cusp, observed in Fig. 8, should be the important feature to confirm the existence of the $\Lambda(1405)$ in the decay of $\chi_{c0} \to \bar{\Lambda}\Sigma\pi$. Thus, we strongly encourage measuring the $\pi\Sigma$ invariant mass distribution of the $\chi_{c0} \to \bar{\Lambda}\Sigma\pi$ decay.

To check the existence of the $\Sigma(1430)$ and $\Sigma(1380)$, we also present the $\pi\bar{\Lambda}$ invariant mass distribution of Fig. 9, where we can see that there is a clear bump structure around 1380 MeV, which is associated to the intermediate resonance $\Sigma(1380)$, and a clear cusp structure around the $\bar{K}N$ threshold, which comes from the $\pi\bar{\Lambda}$ final-state interaction, as shown in Eq. (6). By varying the value of the normalization α as depicted in Fig. 10, the bump structure of $\bar{\Sigma}(1380)$ becomes smoother for a smaller α and more clear

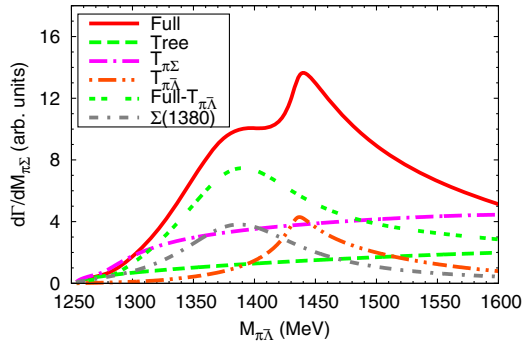

FIG. 9. The $\pi\bar{\Lambda}$ mass distribution of the process $\chi_{c0} \to \bar{\Lambda}\Sigma\pi$. The curve labeled "Full-$T_{\pi\bar{\Lambda}}$" corresponds to our full results excluding the contribution of the $\bar{\Sigma}(1430)$. The explanations of the other curves are same as those of Fig. 6.

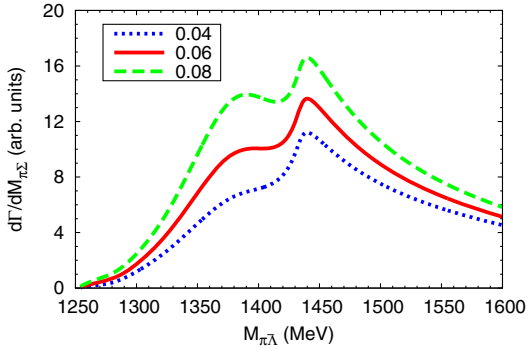

FIG. 10. The $\pi\bar{\Lambda}$ mass distribution of the process $\chi_{c0} \to \bar{\Lambda}\Sigma\pi$ for different values of α of Eq. (8).

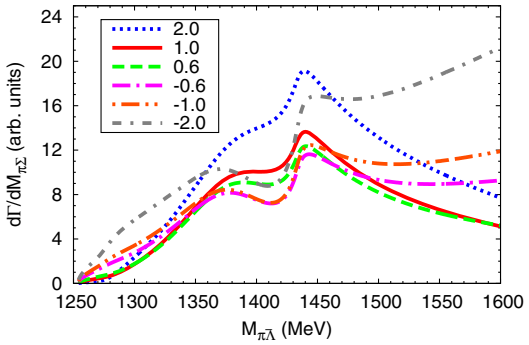

FIG. 11. The $\pi\bar{\Lambda}$ mass distribution of the process $\chi_{c0} \to \bar{\Lambda}\Sigma\pi$ for different values of the ratio R.

for a larger one. It should be stressed that the bump structure of $\bar{\Sigma}(1380)$, or the cusp structure around the $\bar{K}N$ threshold, if confirmed experimentally, should be related to the resonance $\Sigma(1380)$ or $\Sigma(1430)$.

In Fig. 11, we show the $\pi\bar{\Lambda}$ invariant mass distributions by varying the ratio R from -2 to 2. As we can see, the peak structure of the $\bar{\Sigma}(1380)$ and the cusp structure around the $\bar{K}N$ threshold are always clear for different values of the ratio R.

In addition, the $\bar{\Lambda}\Sigma$ states can also process the final-state interaction, which could give rise to some sharp structure (for instance, cusp) at the $\bar{\Sigma}\Sigma$ threshold, and induce some reflection effect on the $\pi\Sigma$ and $\pi\bar{\Lambda}$ invariant mass distributions. By looking at the Dalitz plots of the $\chi_{c0} \to \bar{\Lambda}\Sigma\pi$ process, as shown in Fig. 12, we find that the sharp

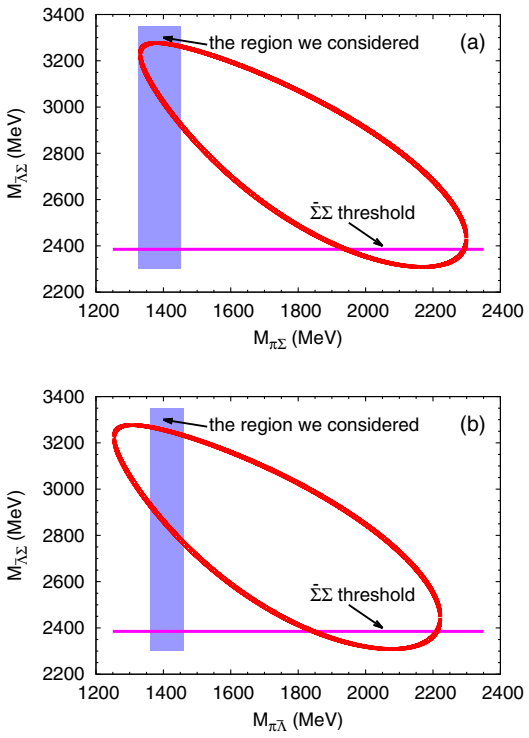

FIG. 12. The Dalitz plots for the $\chi_{c0} \to \bar{\Lambda}\Sigma\pi$ process.

structure around $\bar{\Sigma}\Sigma$ in the $\bar{\Lambda}\Sigma$ distribution only contributes to the $\pi\Sigma$ and $\pi\bar{\Lambda}$ invariant mass distribution 400–500 MeV beyond the regions of the $\Lambda(1405)$ and the Σ^*. Indeed, we have discussed the effect of the sharp structure around the $\bar{\Sigma}\Sigma$ threshold on the $\pi\Sigma$ invariant mass distribution in the $\chi_{c0} \to \bar{\Sigma}\Sigma\pi$ process in Ref. [42], a reaction similar to the present one, and show that the structure of $\pi\Sigma$ invariant mass distribution remains unchanged. Thus, the sharp structure around the $\bar{\Sigma}\Sigma$ threshold should have no significant effect on our predictions and can be safely neglected in here.

So far, we have considered only two-body interactions of the final three particles. It is known that the three-body dynamics plays also a major and sometimes dominant role in the understanding of hadronic resonances [58–61] However, including such contributions, the decay amplitudes would become more complex due to additional parameters, and we cannot determine or constraint these parameters, since there are no experimental data on the $\chi_{c0}(1P) \to \bar{\Lambda}\Sigma\pi$ decay. Hence, we will leave these contributions to future studies when experimental data become available.

Finally, it should be noted that the SIDDHARTA measurement of kaonic hydrogen gives an accurate constraint on the $K^- p$ scattering length [62], and the interaction kernel with the next-to-leading-order chiral perturbation theory is used with the systematic χ^2 analysis in Refs. [13,15,16,63–66] (the important theoretical input for a reliable analysis of SIDDHARTA data can be seen in Ref. [67]). However, for a motivation for measuring this process experimentally, we use the model of the final-state interaction of the $\pi\Sigma$ of $I = 0$ developed in Ref. [22], which can also produce the main feature of the amplitudes of $\pi\Sigma \to \bar{K}N$ and $\pi\Sigma \to \pi\Sigma$ given by the more accurate model.

IV. CONCLUSIONS

In this paper, we have studied the process $\chi_{c0}(1P) \to \bar{\Lambda}\Sigma\pi$ by taking into account the final-state interactions of $\pi\Sigma$ and $\pi\bar{\Lambda}$ within the chiral unitary approach. As the isospin $I = 0$ filter in the $\pi\Sigma$ system and the isospin $I = 1$ filter in the $\pi\bar{\Lambda}$ system, this process can be used to study the molecular structure of the $\Lambda(1405)$ state and to search for the predicted states $\Sigma(1380)$ or $\Sigma(1430)$ with $J^P = 1/2^-$. We have shown that there is a peak of 1350–1400 MeV and a cusp around the $\bar{K}N$ in the $\pi\Sigma$ mass distribution, which should be the important feature of the molecular state $\Lambda(1405)$.

Indeed, the intermediate $\bar{\Sigma}(1385)$ state cannot be fully suppressed because SU(3) symmetry is known be substantially broken. If a bump is observed around 1380 MeV in the $\pi\bar{\Lambda}$ invariant mass distribution, one cannot be 100% sure it comes from the $\bar{\Sigma}(1380)$ resonance, since we do not know the extent to which the $\Sigma(1385)$ is not suppressed. However, the width of $\Sigma(1385)$ (about 40 MeV) is smaller than that of the $\Sigma(1380)$ (120 MeV as predicted), so the corresponding bump structures should have different widths. On the other hand, the decay into $\pi\bar{\Lambda}$ should proceed in the s wave to give rise to the quantum numbers of the $\Sigma(1380)$ and proceed in the p wave to give rise to the ones of the $\Sigma(1385)$. Thus, the partial wave analysis, if the experimental data are available in the future, can also be used to distinguish these two resonances.

In summary, the process $\chi_{c0} \to \bar{\Lambda}\Sigma\pi$ can be used to study the molecular structure of the $\Lambda(1405)$ resonance and also to test the existences of the predicted states $\Sigma(1380)$ and $\Sigma(1430)$.

ACKNOWLEDGMENTS

We thank the anonymous referee for the critical comments that were valuable in improving the presentation of this work. We warmly thank Eulogio Oset for careful reading this paper and useful comments. This work is partly supported by the National Natural Science Foundation of China under Grants No. 11505158, No. 11605158, No. 11475227, and No. 11735003. It is also supported by the Academic Improvement Project of Zhengzhou University.

[1] E. Klempt and J. M. Richard, Baryon spectroscopy, Rev. Mod. Phys. **82**, 1095 (2010).
[2] V. Crede and W. Roberts, Progress towards understanding baryon resonances, Rep. Prog. Phys. **76**, 076301 (2013).
[3] J. A. Oller and U. G. Meißner, Chiral dynamics in the presence of bound states: Kaon nucleon interactions revisited, Phys. Lett. B **500**, 263 (2001).
[4] D. Jido, J. A. Oller, E. Oset, A. Ramos, and U. G. Meißner, Chiral dynamics of the two $\Lambda(1405)$ states, Nucl. Phys. **A725**, 181 (2003).
[5] N. Kaiser, P. B. Siegel, and W. Weise, Chiral dynamics and the low-energy kaon-nucleon interaction, Nucl. Phys. **A594**, 325 (1995).
[6] E. Oset and A. Ramos, Nonperturbative chiral approach to s wave $\bar{K}N$ interactions, Nucl. Phys. **A635**, 99 (1998).
[7] T. Hyodo, S. I. Nam, D. Jido, and A. Hosaka, Flavor SU(3) breaking effects in the chiral unitary model for meson baryon scatterings, Phys. Rev. C **68**, 018201 (2003).
[8] C. Garcia-Recio, J. Nieves, E. R. Arriola, and M. J. V. Vacas, $S = -1$ meson baryon unitarized coupled channel

chiral perturbation theory and the S_{01} $\Lambda(1405)$ and $\Lambda(1670)$ resonances, Phys. Rev. D **67**, 076009 (2003).
[9] C. Garcia-Recio, J. Nieves, and L. L. Salcedo, SU(6) extension of the Weinberg-Tomozawa meson-baryon Lagrangian, Phys. Rev. D **74**, 034025 (2006).
[10] B. Borasoy, R. Nissler, and W. Weise, Chiral dynamics of kaon nucleon interactions, revisited, Eur. Phys. J. A **25**, 79 (2005).
[11] J. A. Oller, On the strangeness -1 S-wave meson baryon scattering, Eur. Phys. J. A **28**, 63 (2006).
[12] B. Borasoy, U. G. Meißner, and R. Nissler, $K^- p$ scattering length from scattering experiments, Phys. Rev. C **74**, 055201 (2006).
[13] Y. Ikeda, T. Hyodo, and W. Weise, Chiral SU(3) theory of antikaon-nucleon interactions with improved threshold constraints, Nucl. Phys. **A881**, 98 (2012).
[14] K. P. Khemchandani, A. M. Torres, H. Kaneko, H. Nagahiro, and A. Hosaka, Coupling vector and pseudoscalar mesons to study baryon resonances, Phys. Rev. D **84**, 094018 (2011).
[15] T. Hyodo and D. Jido, The nature of the $\Lambda(1405)$ resonance in chiral dynamics, Prog. Part. Nucl. Phys. **67**, 55 (2012).
[16] Z.-H. Guo and J. A. Oller, Meson-baryon reactions with strangeness -1 within a chiral framework, Phys. Rev. C **87**, 035202 (2013).
[17] M. Mai and U. G. Meißner, Constraints on the chiral unitary $\bar{K}N$ amplitude from $\pi\Sigma K^+$ photoproduction data, Eur. Phys. J. A **51**, 30 (2015).
[18] S. Prakhov *et al.* (Crystall Ball Collaboration), $K^- p \to \pi^0\pi^0\Sigma^0$ at $p_{K^-} = 514$ MeV/c to 750-MeV/c and comparison with other $\pi^0\pi^0$ production, Phys. Rev. C **70**, 034605 (2004).
[19] V. K. Magas, E. Oset, and A. Ramos, Evidence for the Two Pole Structure of the $\Lambda(1405)$ Resonance, Phys. Rev. Lett. **95**, 052301 (2005).
[20] L. Roca and E. Oset, $\Lambda(1405)$ poles obtained from $\pi^0\Sigma^0$ photoproduction data, Phys. Rev. C **87**, 055201 (2013).
[21] C. Patrignani *et al.* (Particle Data Group), Review of Particle Physics, Chin. Phys. C **40**, 100001 (2016).
[22] L. Roca and E. Oset, Isospin 0 and 1 resonances from $\pi\Sigma$ photoproduction data, Phys. Rev. C **88**, 055206 (2013).
[23] E. Wang, J. J. Xie, W. H. Liang, F. K. Guo, and E. Oset, Role of a triangle singularity in the $\gamma p \to K^+\Lambda(1405)$ reaction, Phys. Rev. C **95**, 015205 (2017).
[24] M. Bayar, R. Pavao, S. Sakai, and E. Oset, Role of the triangle singularity in $\Lambda(1405)$ production in the $\pi^- p \to K^0\pi\Sigma$ and $pp \to pK^+\pi\Sigma$ processes, Phys. Rev. C **97**, 035203 (2018).
[25] J. C. Nacher, E. Oset, H. Toki, and A. Ramos, Photoproduction of the $\Lambda(1405)$ on the proton and nuclei, Phys. Lett. B **455**, 55 (1999).
[26] S. X. Nakamura and D. Jido, $\Lambda(1405)$ photoproduction based on chiral unitary model, Prog. Theor. Exp. Phys. **2014**, 023D01 (2014).
[27] T. Hyodo, A. Hosaka, E. Oset, A. Ramos, and M. J. V. Vacas, $\Lambda(1405)$ production in the $\pi^- p \to K^0\pi\Sigma$ reaction, Phys. Rev. C **68**, 065203 (2003).
[28] J. C. Nacher, E. Oset, H. Toki, and A. Ramos, Radiative production of the $\Lambda(1405)$ resonance in K^- collisions on protons and nuclei, Phys. Lett. B **461**, 299 (1999).
[29] D. Jido, E. Oset, and T. Sekihara, Kaonic production of $\Lambda(1405)$ off deuteron target in chiral dynamics, Eur. Phys. J. A **42**, 257 (2009).
[30] K. Miyagawa and J. Haidenbauer, Precise calculation of the two-step process for $K^- d - > \pi\Sigma N$ in the $\Lambda(1405)$ resonance region, Phys. Rev. C **85**, 065201 (2012).
[31] D. Jido, E. Oset, and T. Sekihara, The $K^- d \to \pi\Sigma n$ reaction revisited, Eur. Phys. J. A **49**, 95 (2013).
[32] S. Ohnishi, Y. Ikeda, T. Hyodo, and W. Weise, Structure of the $\Lambda(1405)$ and the $K^- d \to \pi\Sigma n$ reaction, Phys. Rev. C **93**, 025207 (2016).
[33] X. L. Ren, E. Oset, L. Alvarez-Ruso, and M. J. V. Vacas, Antineutrino induced $\Lambda(1405)$ production off the proton, Phys. Rev. C **91**, 045201 (2015).
[34] L. S. Geng and E. Oset, The role of the $\Lambda(1405)$ in the $pp \to pK^+\Lambda(1405)$ reaction, Eur. Phys. J. A **34**, 405 (2007).
[35] J. Siebenson and L. Fabbietti, Investigation of the $\Lambda(1405)$ line shape observed in pp collisions, Phys. Rev. C **88**, 055201 (2013).
[36] K. Miyahara, T. Hyodo, and E. Oset, Weak decay of Λ_c^+ for the study of $\Lambda(1405)$ and $\Lambda(1670)$, Phys. Rev. C **92**, 055204 (2015).
[37] L. Roca, M. Mai, E. Oset, and U. G. Meißner, Predictions for the $\Lambda_b \to J/\psi\Lambda(1405)$ decay, Eur. Phys. J. C **75**, 218 (2015).
[38] N. Ikeno and E. Oset, Semileptonic Λ_c decay to νl^+ and $\Lambda(1405)$, Phys. Rev. D **93**, 014021 (2016).
[39] J. J. Xie, W. H. Liang, and E. Oset, Hidden charm pentaquark and $\Lambda(1405)$ in the $\Lambda_b^0 \to \eta_c K^- p(\pi\Sigma)$ reaction, Phys. Lett. B **777**, 447 (2018).
[40] L. R. Dai, R. Pavao, S. Sakai, and E. Oset, Anomalous enhancement of the isospin-violating $\Lambda(1405)$ production by a triangle singularity in $\Lambda_c \to \pi^+\pi^0\pi^0\Sigma^0$, Phys. Rev. D **97**, 116004 (2018).
[41] J. J. Xie and E. Oset, Search for the Σ^* state in $\Lambda_c^+ \to \pi^+\pi^0\pi^-\Sigma^+$ decay by triangle singularity, arXiv:1811.07247.
[42] E. Wang, J. J. Xie, and E. Oset, $\chi_{c0}(1P)$ decay into $\bar{\Sigma}\Sigma\pi$ in search of an $I = 1$, $1/2^-$ baryon state around $\bar{K}N$ threshold, Phys. Lett. B **753**, 526 (2016).
[43] A. Zhang, Y. R. Liu, P. Z. Huang, W. Z. Deng, X. L. Chen, and S. L. Zhu, $J^P = 1/2^-$ pentaquarks in Jaffe and Wilczek's diquark model, HEPNP **29**, 250 (2005).
[44] B. S. Zou, Penta-quark components in baryons and evidence at BES, Int. J. Mod. Phys. A **21**, 5552 (2006).
[45] B. S. Zou, On the nature of the lowest $1/2^-$ baryon nonet and decuplet, Eur. Phys. J. A **35**, 325 (2008).
[46] J. J. Wu, S. Dulat, and B. S. Zou, Evidence for a new Σ^* resonance with $J^P = 1/2^-$ in the old data of $K^- p \to \Lambda\pi^+\pi^-$ reaction, Phys. Rev. D **80**, 017503 (2009).
[47] J. J. Wu, S. Dulat, and B. S. Zou, Further evidence for the Σ^* resonance with $J^P = 1/2^-$ around 1380-MeV, Phys. Rev. C **81**, 045210 (2010).
[48] J. J. Xie, J. J. Wu, and B. S. Zou, Role of the possible $\Sigma^*(\frac{1}{2}^-)$ state in the $\Lambda p \to \Lambda p\pi^0$ reaction, Phys. Rev. C **90**, 055204 (2014).
[49] J. J. Xie and L. S. Geng, $\Sigma^*_{1/2^-}(1380)$ in the $\Lambda_c^+ \to \eta\pi^+\Lambda$ decay, Phys. Rev. D **95**, 074024 (2017).
[50] R. G. Edwards, N. Mathur, D. G. Richards, and S. J. Wallace (Hadron Spectrum Collaboration), Flavor structure of the

excited baryon spectra from lattice QCD, Phys. Rev. D **87**, 054506 (2013).
[51] G. P. Engel, C. B. Lang, D. Mohler, and A. Schäfer, Excited light and strange hadrons from the lattice with two chirally improved quarks, Proc. Sci., Hadron2013 (**2013**) 118.
[52] G. P. Engel, C. B. Lang, D. Mohler, and A. Schäfer (BGR Collaboration), QCD with two light dynamical chirally improved quarks: Baryons, Phys. Rev. D **87**, 074504 (2013).
[53] E. Oset, A. Ramos, and C. Bennhold, Low lying $S = -1$ excited baryons and chiral symmetry, Phys. Lett. B **527**, 99 (2002); **530**, 260(E) (2002).
[54] L. R. Dai, J. M. Dias, and E. Oset, Disclosing $D^*\bar{D}^*$ molecular states in the $B_c^- \to \pi^- J/\psi\omega$ decay, Eur. Phys. J. C **78**, 210 (2018).
[55] E. Wang, J. J. Xie, L. S. Geng, and E. Oset, Analysis of the $B^+ \to J/\psi\phi K^+$ data at low $J/\psi\phi$ invariant masses and the $X(4140)$ and $X(4160)$ resonances, Phys. Rev. D **97**, 014017 (2018).
[56] E. Wang, J. J. Xie, L. S. Geng, and E. Oset, The $X(4140)$ and $X(4160)$ resonances in the $e^+e^- \to \gamma J/\psi\phi$ reaction, arXiv:1806.05113.
[57] L. R. Dai, G. Y. Wang, X. Chen, E. Wang, E. Oset, and D. M. Li, The $B^+ \to J/\psi\omega K^+$ reaction and $D^*\bar{D}^*$ molecular states, arXiv:1808.10373.
[58] M. Mai, B. Hu, M. Döring, A. Pilloni, and A. Szczepaniak, Three-body unitarity with isobars revisited, Eur. Phys. J. A **53**, 177 (2017).
[59] M. Mai and M. Döring, Three-body unitarity in the finite volume, Eur. Phys. J. A **53**, 240 (2017).
[60] M. Mai, B. Hu, M. Döring, A. Pilloni, and A. Szczepaniak, Three-body scattering in isobar ansatz, Proc. Sci., Hadron2017 (**2018**) 140.
[61] M. Döring, H. W. Hammer, M. Mai, J.-Y. Pang, A. Rusetsky, and J. Wu, Three-body spectrum in a finite volume: The role of cubic symmetry, Phys. Rev. D **97**, 114508 (2018).
[62] M. Bazzi *et al.*, Kaonic hydrogen X-ray measurement in SIDDHARTA, Nucl. Phys. **A881**, 88 (2012).
[63] M. Mai and U. G. Meißner, Constraints on the chiral unitary $\bar{K}N$ amplitude from $\pi\Sigma K^+$ photoproduction data, Eur. Phys. J. A **51**, 30 (2015).
[64] M. Mai and U. G. Meißner, New insights into $\bar{K}N$ scattering and the structure of the $\Lambda(1405)$, Nucl. Phys. **A900**, 51 (2013).
[65] M. Mai, Status of the $\Lambda(1405)$, Few-Body Syst. **59**, 61 (2018).
[66] M. Mai, V. Baru, E. Epelbaum, and A. Rusetsky, Recoil corrections in $\bar{K}$-deuteron scattering, Phys. Rev. D **91**, 054016 (2015).
[67] U. G. Meißner, U. Raha, and A. Rusetsky, Spectrum and decays of kaonic hydrogen, Eur. Phys. J. C **35**, 349 (2004).